

Analysis of Excitation Behavior of Two-Stage Gearbox Based Upon Validated Simulation Model

Christian Brecher, Christoph Löpenhaus and Marius Schroers

In order to reduce costs for development and production, the objective in gearbox development and design is to predict running and noise behavior of a gearbox without manufacturing a prototype and running expensive experimental investigations. To achieve this objective, powerful simulation models have to be set up in a first step. Afterwards, those models have to be qualified and compared to experimental investigations. During the investigation procedure of gearboxes, there are two possibilities to evaluate the running and noise behavior: quasi-static and dynamic investigations. In times of engine downsizing, e-mobility and lightweight design, the dynamic excitation behavior is becoming increasingly important. Opposed to the quasi-static excitation, the dynamic excitation behavior of the gearbox regards increased load at resonance points caused by the dynamic behavior of the complete drive train.

The dynamic behavior of one-stage gearboxes has been the subject of scientific research for many years. In contrast, there have been few reports which investigate the running behavior of multi-stage gearboxes in the last few years. Most of them are based on computational investigations. However, to utilize the results of those simulation models for design purposes, it is indispensable to compare simulation results with experimental results.

Additionally, the objective of this paper is the analysis of the excitation behavior and the development of a simulation model for a two-stage gearbox. Based on a reference test variant, several gear parameters, such as helix angle and number of teeth, are varied in both stages by changing the gears and are investigated. Subsequently, a simulation model is presented which is able to calculate the dynamic excitation behavior of the two-stage gearbox tests.

Introduction

Multi-stage cylindrical gearboxes are used in the entire drive train technology. In addition to a sufficient load capacity and high gearbox efficiency, the acoustic behavior has to be taken into account. The increasing demands on the acoustic behavior appear in customer requirements and amended law restrictions, e.g., in automotive or wind industry (Refs. 21; 19). For a single-stage gearbox, several research projects have been carried out (Refs. 3–4; 13; 15–16). Because of the mutual interactions between the gear meshes at a two-stage gearbox, the knowledge cannot be transferred directly without restrictions.

The excitation behavior of gearboxes is mainly determined by the gear mesh excitation. A selection of influence factors is shown in Figure 1. In order to reduce the parametric excitation, an integer contact ratio is recommended by changing, for example, the helix angle or the face width (Ref. 23). On the one hand, flank modifications influence the path-dependent excitation. On the other hand,

they are often used to reduce the impact excitation. The consideration of parametric, path-dependent and impact excitation in the acoustic-oriented design of single-stage gearboxes is state of the art, especially for quasi-static and partly for dynamic conditions (Refs. 11; 16–17).

For multi-stage gearboxes, additional parameters have to be taken into account. Firstly, the gears of the first stage enter mesh related to the line of action. Due to the gear geometry, the time when the gears of the second stage enter mesh is mostly temporally displaced. This phenomenon is called phase shift. Furthermore, the stiffness of the connecting shaft between the gear meshes influences the interaction of the single gear stages. Due to a differing number of teeth in the two stages, the noise behavior of the entire gearboxes changes, as well. In this report, the influence of the phase shift between the gear meshes is investigated by means of calculations. Hence, discrete values of the phase shift are inserted and investigated. The calculation procedure was validated based

on tests with a single-stage gearbox and enhanced to a two-stage gearbox.

State of the Art

The excitation behavior of single-stage gearboxes is topic of many research activities (Refs. 3–4; 13; 15–16). Based on these researches, there are scientific publications dealing with multi-stage gearboxes. Mostly, the excitation behavior is discussed by means of calculated theoretical models and rarely compared with empiric investigations.

Gold conducts numerical and experimental investigations with three-stage gearboxes. Hence, he develops a vibration model using only the torsional degree of freedom. This model is extended to a spatial system using all six degrees of freedom to perform a dynamic analysis. His work indicates the necessity of spatial simulation models to identify the Eigen frequencies of multi-stage gearboxes. Only in special cases can the lowest Eigen frequencies be calculated by using torsional vibration models. In order to get results close to reality, the coupled

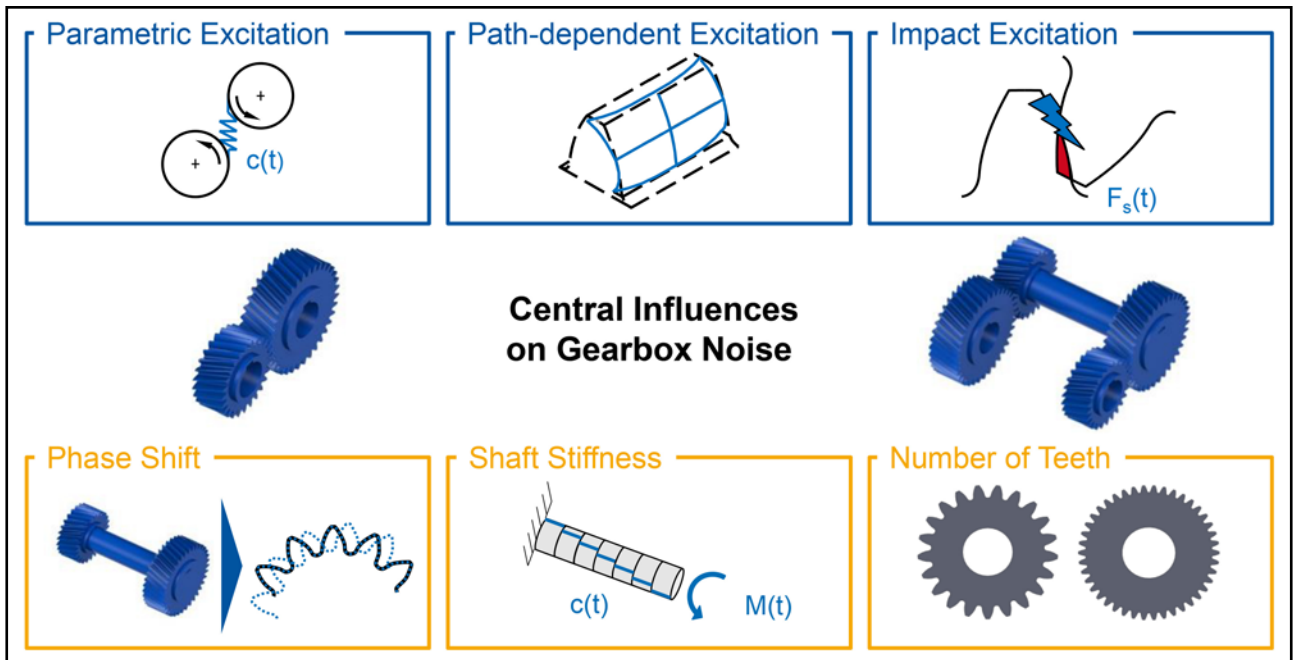


Figure 1 Central Influences on Gearbox Noise.

elements like shafts and machinery have to be included in calculation (Ref. 9).

Vinayak et al. describe the equation of motion for single-stage gearboxes, including all six spatial degrees of freedom. The simulation model is expanded to analyze a gear chain using three gears and a two-stage gearbox. There is an investigation of the model using temporal variable (*LTV*=linear time variant) and temporal constant parameters (*LTI*=linear time invariant). The numerical results show the existence of an interaction between the gear meshes (Ref. 20).

Sattelberger investigates the dynamic behavior of single- and two-stage cylindrical gearboxes by means of experimental and mathematical results. The focus of his analysis includes coupling stiffness and phase shift between both gear meshes. Concerning the coupling stiffness, he discovers that the gear meshes are not affected by each other for a low coupling stiffness. In contrast, for a high stiffness, the stiffness between individual gear meshes can be relevant. Regarding identical or similar tooth contact frequencies of the gear meshes, the adaption of a phase shift of a half pitch is usable for excitation reduction. This result can be confirmed by a parallel connection of two cylindrical gears that are distorted a half pitch against each other (Ref. 18).

The results of Sattelberger are verified by the investigations of Cheon. In his paper he also studies the phase shift

mathematically by parallel connection of two cylindrical gears. The model has a minimum of excitation when the cylindrical gears are distorted a half-pitch against each other (Ref. 5).

Kuber et al. also use a model with six degrees of freedom for theoretical analysis of multi-stage gearboxes, which can contain any number of gears. The model is validated through experimental results of a single-stage gearbox. Subsequently several parameters are varied on the basis of a two-stage gearbox. The effect of the change of the intermediate shaft length, the bearing stiffness, the phase shift, and the orientation of the helix angle on the tooth and bearing force is evaluated (Ref. 12).

Zhou et al. conduct acoustical research on two-stage gearboxes — theoretically and experimentally. The comparison between measurement and simulation shows good correlation. Additional to the gear mesh frequency, there are also modulation frequencies that indicate an interaction between the gear meshes. The analysis of the appearing orders identifies the gear mesh responsible for the modulation (Ref. 22).

Hesse investigates the excitation behavior through variation of gear mesh excitation experimentally. The gear mesh excitation is varied by changing the topography of the tooth surface. The analyzed test setup consists of a manual gearbox. Together with the gear stage on the coun-

Table 1 Nomenclature	
b_f	Face Width
i	Gear Ratio
m_n	Module
n_{in}	Rotational Speed
T_{in}	Torque
z_1/z_2	Number of Teeth
α_n	Pressure Angle
β_1/β_2	Helix Angle
ϵ_α	Contact Ratio
ϵ_β	Overlap Ratio

tershaft, the setup matches a two-stage gearbox. The gearbox is connected by a constant velocity joint shaft to the hypoid gear stage. Because of the large distances between the stages and the influence of the drive train stiffness, there are minor interactions between the gear meshes. According to this, the behavior of the drive train elements between gear sets has significant influence (Ref. 10).

As the state of the art shows, the minority of the reports focuses on the dynamic excitation behavior of two-stage gearboxes. Furthermore, there are fewer reports which regard the dynamic interactions between the different influences on noise behavior of two-stage gearboxes mathematically as well as experimentally.

Objective and Approach

The objective and the approach of this paper are presented in Figure 2. The objective is the evaluation of dynamic excitation behavior of two-stage gearboxes with a focus on phase shift. For this

reason, a two-stage test gearbox is developed and designed based on an existing single-stage gearbox. In order to analyze the excitation as well as noise behavior, measurement equipment is integrated in the test setup to detect the machine-acoustic noise generation. For single-stage gearboxes, a simulation model is presented. The simulation model of the single-stage gearbox is validated with experimental results. Based on this model and its parameters, an enhanced model is developed which enables analysis of the dynamic behavior of two-stage gearboxes.

Consequently, the model is used to analyze the influence of dynamic interactions on the excitation behavior. Thereby, the focus of this analysis is on the phase shift between the gear meshes.

Test Setup and Test Specimen

For the investigations of this work, both test gearboxes in Figure 3 are taken into account. The setup of the single-stage gearbox is described in detail (Ref. 4). Based on this concept a two-stage gearbox prototype has been developed. The central component of the gearbox is the

housing, which is constructed in a shell construction of upper and lower shell. For easier handling during assembly, the upper shell is manufactured in two parts. The housing is mounted on damping elements in order to decouple vibrations of the test rig. To change the emission characteristics of the test gearbox, the strength of the thin-walled side elements can be varied.

The shafts with the bearings are mounted through bushings in the housing. The tapered roller bearings are designed in X-arrangement. By cover

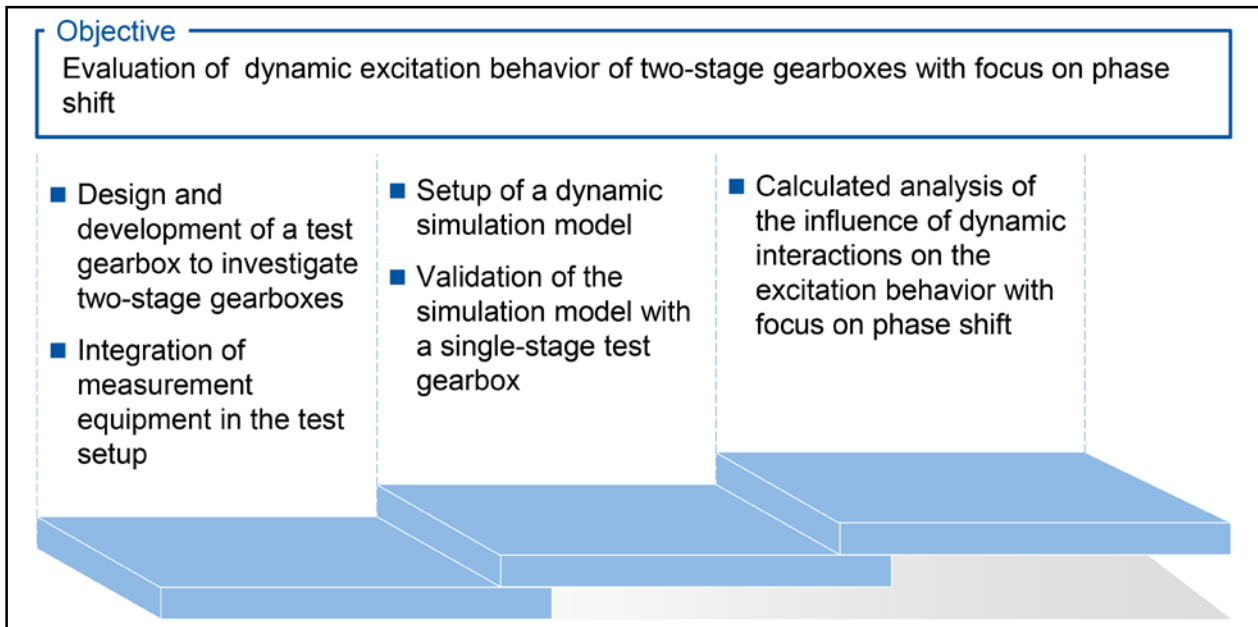


Figure 2 Objective and Approach.

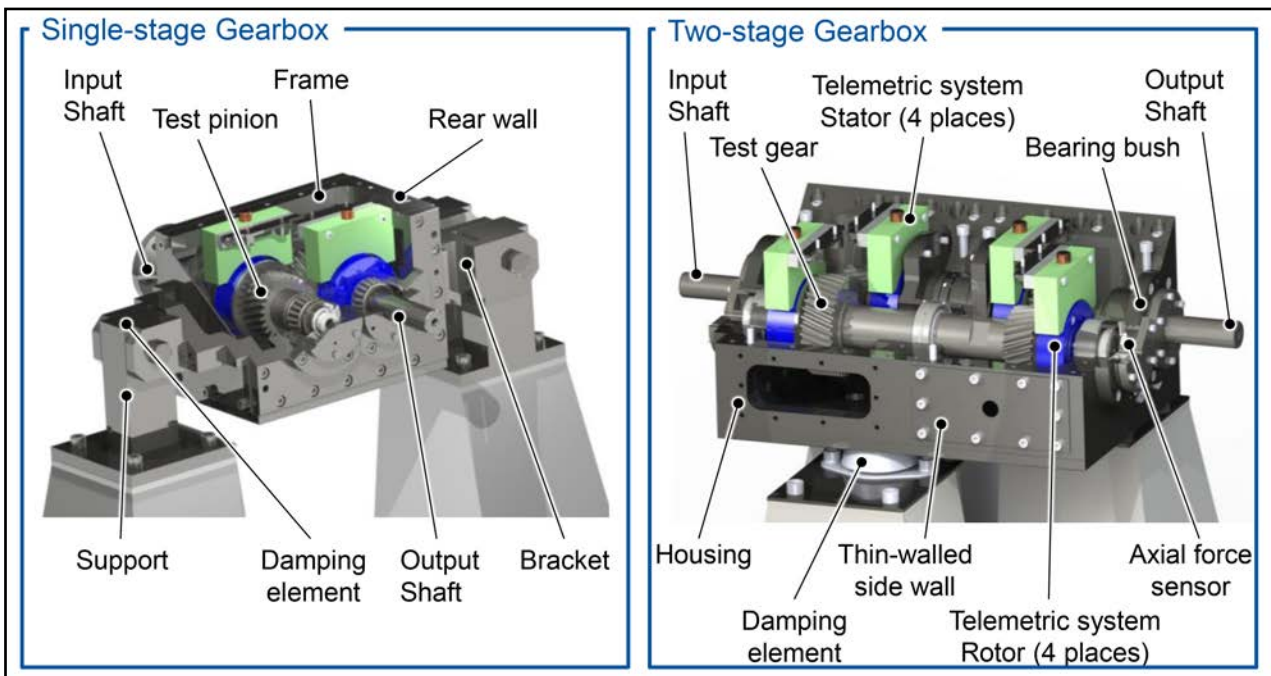


Figure 3 Design of the Test Gearboxes.

plates, the bearing pre-load can be adjusted. A piezoelectric force sensor can be integrated in the test setup. Thereby, it is possible to flexibly measure and adjust the axial pre-load force of the tapered roller bearings. Furthermore, a support bearing can be mounted optionally on the connecting shaft between the gear meshes in order to reduce the bending of the shaft. During the investigations, gears with the same macro geometry are mounted at each gear stage (Table 2). In the bottom plate, the exhaust system for the oil sump of the injection lubrication is mounted. An external unit with a constant temperature-controlled tank supplies the oil. The supply of oil to the gear meshes is realized via a pipe duct to the rear wall of the test gearbox and a tangential injection into the incoming gear mesh. The bearings are supplied via pipe ducts with oil as well. The flow distribution was adjusted to an optimal supply.

To analyze the excitation and noise behavior of the gearboxes, different measurement equipment is integrated in the test setups. Figure 4 gives an overview. The measurement equipment is divided into three groups along the machine-acoustic noise generation: source, path and receiver. Firstly, the source of the excitation is represented by the gear mesh. In principle, the gear mesh excitation can be analyzed by measuring dynamic tooth force, tooth root strain or

torsional vibrations. The first two methods mentioned are not feasible, due to either the difficult realization or to design limitations. Therefore, the torsional vibration measurement has been established to measure the gear mesh excitation (Refs. 2; 14). Hence, the angular acceleration of each shaft is measured. In (Ref. 7) the angular acceleration is converted in a translational differential acceleration in the line of action using Equation 1. For an adequate characterization of the excitation, the position of the angular measurement systems is to choose the closest to the gear mesh as possible (Ref. 10).

$$\Delta \ddot{A} = r_{b2} \cdot \ddot{\varphi}_2(t) - r_{b1} \cdot \ddot{\varphi}_1(t) \quad (1)$$

where

$\Delta \ddot{A}$ is difference acceleration

r_{bi} is base circle

$\ddot{\varphi}_i$ is angular acceleration

The angular measurement systems are integrated into the test setup; see Figure 4 on the right. These consist of a rotor, which is co-rotating with the shaft, and a stator, which is fixed to the housing. On the rotor, two acceleration sensors with an offset of 180° are mounted. By adding the acceleration signals of both sensors, radial vibration components can be compensated and only the tangential acceleration is measured. The power supply is provided via the inductive coil. Following the machine-acoustic noise generation in Figure 4 on the left, the next step is the

structure-borne noise.

The structure-borne noise is measured on the surface of the gearbox housing with accelerometers. Due to the large surfaces, it is not possible to measure the structure-borne noise simultaneously at all surfaces. Therefore, single measurement points are selected as reference points according to (Ref. 8).

The last step of the machine-acoustic noise generation is the receiver. The received airborne noise is measured under free field conditions with electrostatic microphones. Hence, five microphones are placed around the gearbox. Four microphones are in the axis plane of the gearbox. The last microphone is placed above the gearbox with the same distance. Thus, the five microphones describe a cuboid.

Table 2 gives an overview over the gear sets whose influence on the excitation behavior is to be evaluated in this paper. All gear sets can be manufactured with the same tool. Therefore, all gear sets have the same pressure angle $\alpha_n = 20^\circ$ and module $m_n = 3.5 \text{ mm}$. The face width of all gears is equal as well. The variants vary in the helix angle and the number of teeth. Gear sets 1 and 3 are helical gears with a helix angle of $\beta = 19.3^\circ$ (Ref. 1) and $\beta = 20^\circ$ (Ref. 3). Gear set 2 is a spur gear ($\beta = 0.0^\circ$). Gear set 1's gears have 25 and 36 teeth, which leads to a gear ratio of $i = 1.44$. The gear sets 2 and 3 have an

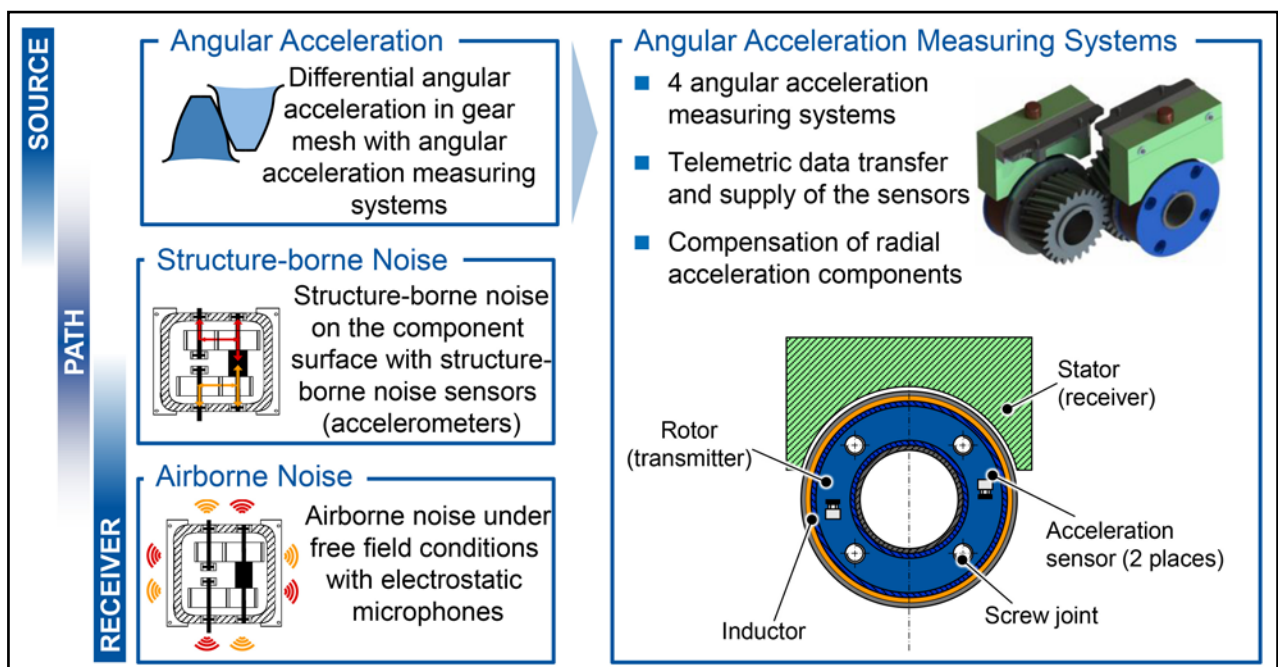


Figure 4 Measurement Equipment.

identical number of teeth for both gears and therefore a gear ratio of $i=1$. For the two-stage gearboxes, gears with the same macro geometry are mounted at both gear stages, as mentioned before.

Setup and Validation of the Dynamic Simulation Model

Due to varying requirements and working conditions during the operational use of gearboxes, the operating conditions (for example torque and rotational speed) are not constant. For special operational points, the overload can be critical for the load carrying capacity and the excitation behavior. Mostly, the critical operational points occur when the excitation frequencies coincide with Eigen frequencies of the test setup. In this case, a quasi-static investigation is not effective, and a dynamic analysis is necessary. For both test gearboxes shown in Figure 3, a similar approach to build up a dynamic simulation model is selected. Figure 5 illustrates the two main components and their interaction. The force coupling elements represent the gear mesh, and the drive train model includes the properties of the gearbox and the entire drive train.

The force coupling element requires a subroutine of the tooth contact analysis FE-Stirnradkette (STIRAK) that is developed at WZL (Ref. 1). STIRAK enables the calculation of excitation maps based on input data; see Figure 5. As data is put in the gearbox structure, the macro

and micro geometry of the gears and tool data, for example, the properties of the tooth flank can be set via nominal data or be imported either by data of a manufacturing simulation or by real measurement data. Based on the input data, a spring model is set up and solved. As a result, the excitation maps are obtained. Depending on the load-dependent transmission error and the current angular position of the gear, actual excitation forces and torques can be determined.

The approach to build up the drive train model is presented in Figure 5 on the right. The objective of this step is to provide the system matrices for the simulation (inertia, stiffness, and damping). In this paper, only the torsional degree of freedom is regarded. Due to the domination of rotational excitation of the gear mesh, this assumption is suitable (Ref. 4). In order to identify realistic Eigen frequencies and Eigen modes of the test setup, a model of the complete test rig is regarded. The setup contains the motor and the generator and includes each

part between the two machines, such as the gearbox and constant velocity joint shafts. The first step in the approach to design the drive train model in Figure 5 is the discretization. In this step, the drive train is divided into discrete inertias. Each inertia is connected to its neighboring inertias by massless spring-dampener units. The closer a mass is placed to the gear mesh, the more finely it is discretized to accurately represent the vibrational behavior near the gear meshes. Subsequently, the numerical values of the parameters are determined. Simple components can be parameterized using analytical equations. Furthermore, the inertia of the non-cylindrical components can be extracted from CAD models. However, some parameters are difficult to calculate, such as the contact stiffness of frictional connections, form closures, and damping. An iterative procedure has been established to compare measurement and simulation results when setting parameters for these components.

The first two steps of the approach

Table 2 Investigated Gear Sets				
		Gear Set 1	Gear Set 2	Gear Set 3
Pressure Angle	a_n	20°	20°	20°
Module	m_n	3.5 mm	3.5 mm	3.5 mm
Helix Angle	β_1/β_2	-19.3/19.3°	0°	-20/20°
Gear Ratio	i	1.44	1	1
Number of Teeth	z_1/z_2	25/36	32/32	30/30
Tooth Width	b_1/b_2	41.5/44 mm	41.5/44 mm	41.5/44 mm
Contact Ratio	ϵ_α	1.75	1.7	1.6
Overlap Ratio	ϵ_β	1.25	0	1.3

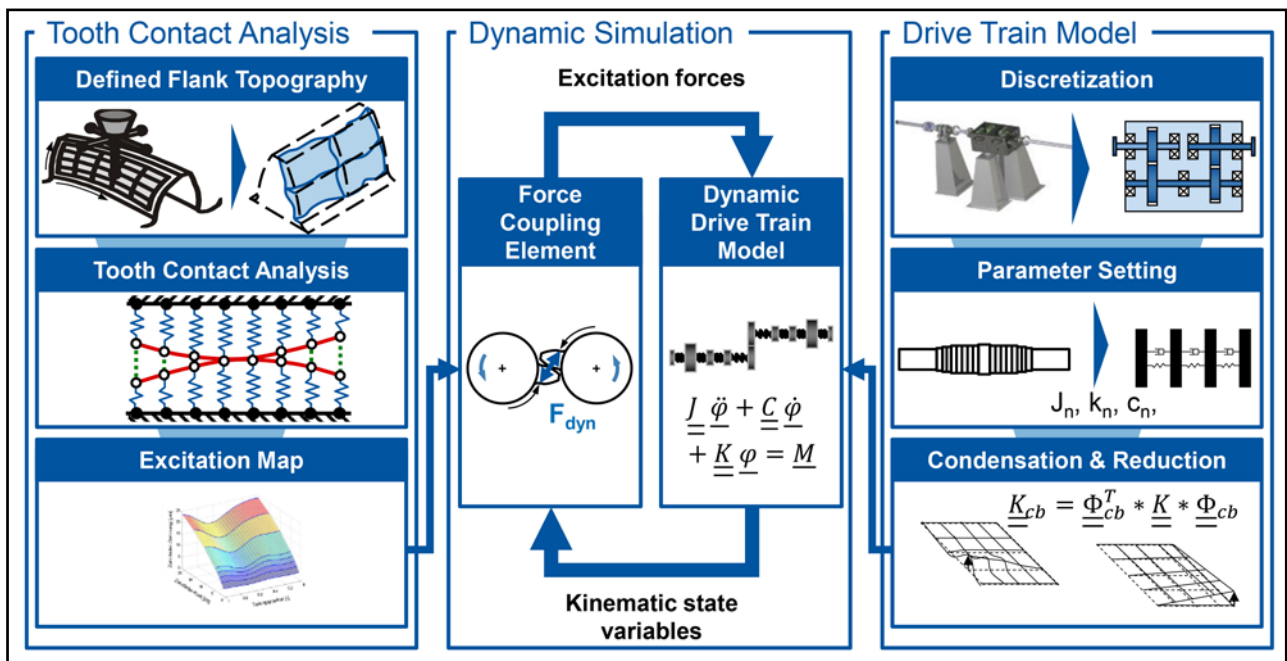


Figure 5 Components of the Dynamic Simulation Model Referring to [4].

generate models with a high number of degrees of freedom. Hence, the numerical solution of those systems would be uneconomically long, and the numerical accuracy would be decreased. To avoid both disadvantages, a modal reduction of degrees of freedom by Craig and Bampton is performed (Ref. 6). For this procedure, the rotational vibration and the external torques are inserted at the external degrees of freedom. The external and the modal degrees of freedom of the lowest Eigen frequencies can be maintained. The frequencies within the acoustically relevant frequency range are not reduced and only high Eigen frequencies are neglected. Therefore, this reduction method is suitable.

The interaction between the force coupling element and the drive train model is shown in the middle of Figure 5. For each time step, the drive train model transfers the kinematic state variables (angle of rotation and rotational speed) to the force coupling element. Depending on the input data, the force coupling element determines the excitation forces with excitation maps and returns them to the drive train model. The excitation forces are composed of a variable tooth stiffness term and a damping term. The tooth stiffness term is determined by the aforementioned excitation maps from STIRAK. In contrast, the damping term

utilizes a velocity proportional approach. With the excitation forces and the generated system matrices, the differential equations can be solved. This procedure will be repeated for each time step.

For the single-stage gearbox in Figure 3, the comparison between experimental and arithmetical results is shown in Figure 6. Table 1 gives an overview about the symbols used in Figures 6 through 9.

The experimental investigations have been performed on a universal gearbox test rig. For the calculated results, a simulation model referred to in Figure 5 has been developed. For this model, the complete setup has been regarded in the drive train model. The investigations are evaluated for the difference velocity. According to Equation 1, the difference velocity is the integrated difference acceleration. The results are compared for two constant driving torques and rotational speed run-ups from $n_1 = 150 \dots 3,500 \text{ min}^{-1}$. For the averaged frequency spectra in the upper row of Figure 6, there is a high conformity between experimental and simulation results. The averaged frequency spectra enable an identification of the Eigen frequencies of the test setup independent from the rotational speed. Especially for the acoustically sensitive frequency range between 1 and 5 kHz, the amplitudes of the resonance frequencies at 460 Hz, 1,180 Hz and between 3 and

4 kHz correlate well. For the order spectra, the amplitudes of the gear mesh frequencies match well. However, the arithmetical results have greater amplitudes than the experimental results (especially for the higher driving torque). In summary, the validation of the simulation model with the experimental results from the test rig has been successful.

For the two-stage gearbox, a second force coupling element is added. Furthermore, the model setup has to be expanded in order to regard the phase shift between the gear meshes. The phase shift is the temporal offset between the two gear meshes. It is defined as the difference between the points when the gear stages enter mesh (relating to the contact path). Possible numerical values of the phase shift are between 0 and 1 in relation to the beginning point of the first gear mesh. The values 0 and 1 mean a simultaneous beginning of the two gear meshes. For a phase shift between 0 and 1, the gear meshes begin with a temporal offset. The integration of the phase shift in the simulation model takes place in the force coupling element of the second gear mesh. Hence, the drive train model has to be modified as well. The parameter setting is based on the validated model of the single-stage gearbox. Hence, the validated single-stage model has been extended to a two-stage model; compare Figure 3.

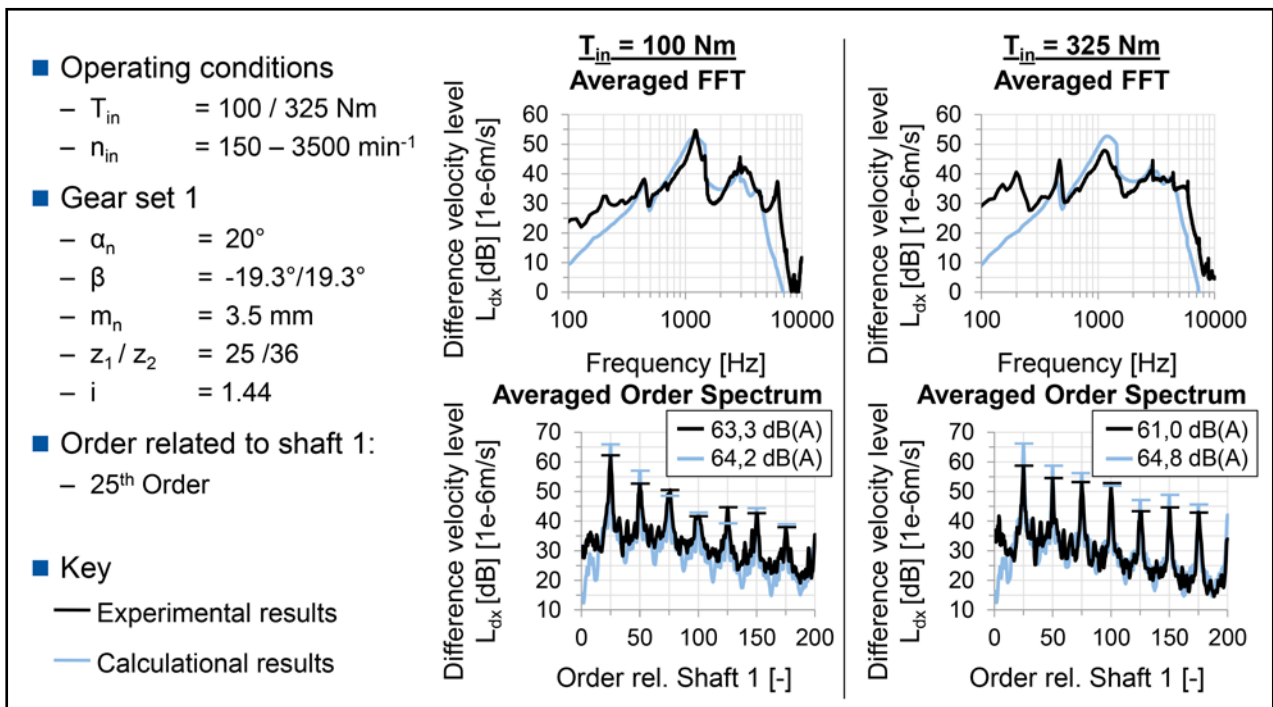


Figure 6 Validation of the Single-Stage Simulation Model [4].

Analysis of Dynamic Excitation Behavior of Two-stage Gearboxes

With the two-stage simulation model introduced in the previous section, the dynamic simulations are performed. Firstly, the excitation behavior of gear set 1 is analyzed. Subsequently, the influence of the phase shift is evaluated by means of the gear sets shown in Table 1. Hence, every gear set is used twice for each of the two stages.

Reference Gear Sets

The simulation model of the single-stage gearbox is validated by means of the experimental results of gear set 1. Therefore, this gear set has been selected as reference gear set for the calculative investigations of the two-stage gearbox as well. In this case, the gear ratio of one stage is $i=1.44$, which leads to total gear ratio $i=2.07$ of the two-stage gearbox. The operating conditions are oriented to the torques and rotational speed of the single-stage gearbox. For the averaged frequency spectrum in the upper

row of Figure 7, the Eigen frequencies of the test setup can be identified. In the left column, the results of the first stage are shown. The results of the second stage are presented on the right. The little sketches in the upper right corner of the averaged frequency spectrums are an indicator for the investigated gear stage. For both stages, the dominant resonance frequencies occur at $f=1,180$ Hz and between 3 and 4 kHz. The frequency spectrum of the single-stage in Figure 6 was dominated by the same resonance frequencies. These frequencies are characterized by frictional connections and form fits inside the gearbox. Due to the unchanged parameters, the frequencies remain the same for both gearboxes. Within the lower frequency range up to 700 Hz, differences between the single- and two-stage test setup occur. The setup, which consists of constant velocity joint shafts and bearings, is slightly changed for the two gearboxes. Those components have a low stiffness. Hence, the differences within the lower frequency range can be

explained. However, a higher excitation can be detected within the acoustic relevant frequency range for the higher driving torque. These differences are more pronounced for the second stage.

For the averaged order spectrum of both stages, both gear mesh orders and their harmonics can be detected. According to the number of teeth, the gear mesh order of the first stage is the 25th order. The order of the second stage is referred to the rotational speed of shaft 1 as well. Therefore, the order of the second stage can be calculated with Equation 2:

$$Ord_{2st} = \frac{n_3 \cdot z_3}{n_1} = \frac{z_3}{i} = 17.4 \quad (2)$$

where

Ord_{2st} is gear mesh order of the second stage

n_i is rotational speed

z_i is number of teeth

i is gear ratio

For the spectrum of the first stage, the first gear mesh order ($=25^{th}$) and its harmonics dominate the spectrum. In con-

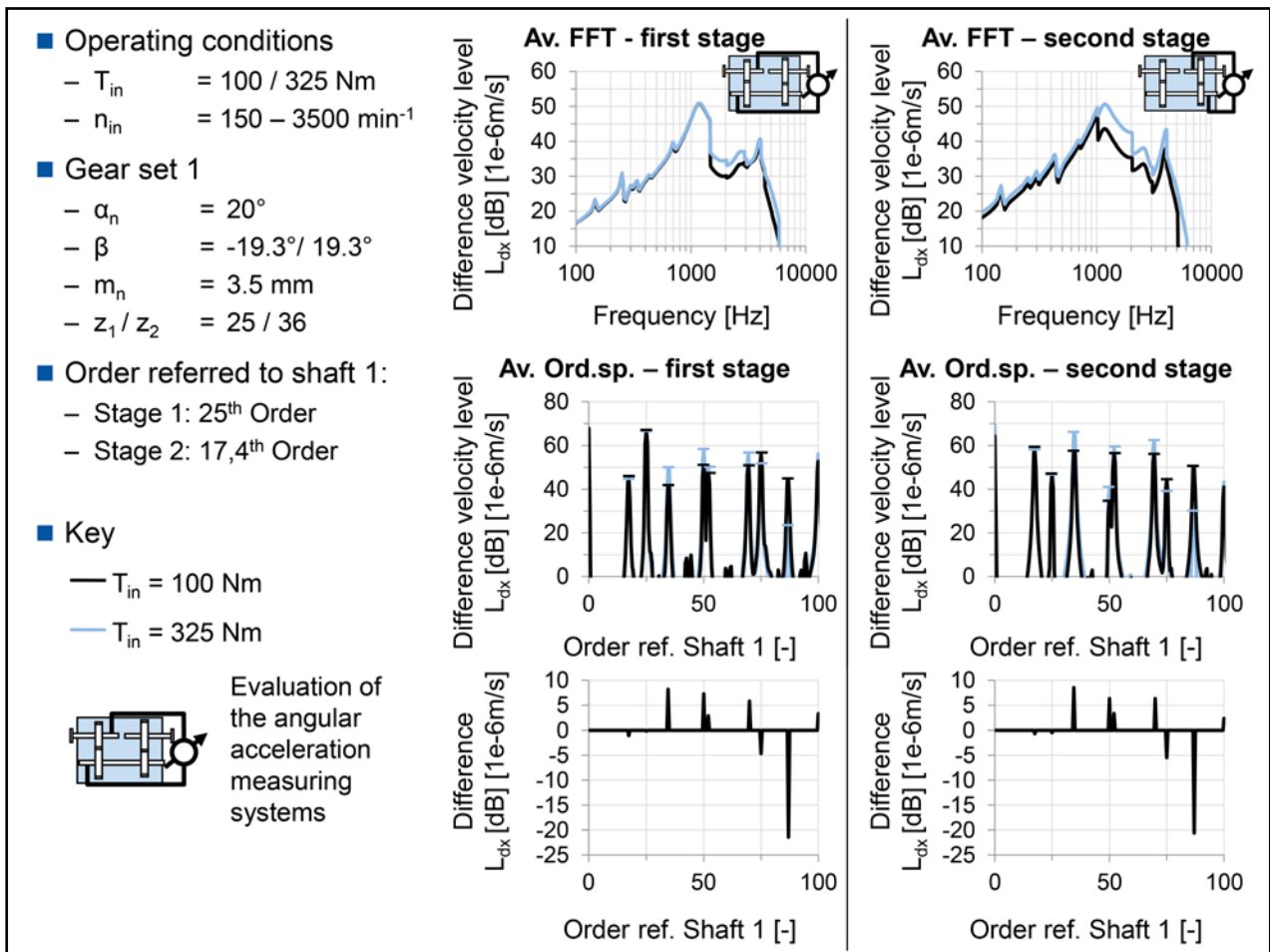


Figure 7 Excitation Behavior of Gear Set 1.

trast, the gear mesh orders of the second stage have greater excitation levels in the spectrum than the orders of the first stage. It is also striking that the second gear mesh order of the first stage (50th order) is very close to the third gear mesh order of the second stage (52.1th order). Within this order range, there is an increased excitation. The differences between the two input torques in the order spectrum are confirmed by means of the last row of Figure 7. Mostly, the orders of the higher excitation torque have a higher excitation level.

Phase Shift

The influence of the phase shift is analyzed with the gear sets shown in Table 1. For this purpose, two configurations of the phase shift are regarded, in which the two gear meshes begin either simultaneously ($p=0$) or by a half pitch offset ($p=0.5$). A compensation by the phase shift on a two-stage gearbox is to be expected when the gears on the intermediate shaft have either an equal number

of teeth or multiples of the numbers of teeth (Ref. 18).

Firstly, gear set 1 is investigated. Hence, the gears on the intermediate shaft have different numbers of teeth (36 and 25). Due to the different number of teeth of both gears on the intermediate shaft, the start of the second gear mesh shifts from tooth to tooth in each pitch relative to the first. Therefore, the phase shift does not reach a constant value. The aforementioned parameters for the phase shift are only valid at the beginning of the simulation. Due to that fact, no influence of a phase shift on the difference velocity level at the reference gear set is expected. Figure 8 confirms this expectation. For the averaged frequency spectrum, the average order spectrum, and the difference in the order spectrum of the first and the second stage, no deviations can be noted.

Therefore, two alternative gear sets with a gear ratio $i=1$ have been designed (for gear data, see Table 1). Hence, the two gears on the intermediate shaft have

the same number of teeth. Gear set 2 has a helix angle $\beta=0^\circ$, and gear set 2 is a helical gear pair ($\beta=20^\circ$). In difference to the analysis of gear set 1, the excitation behavior of gear set 2 and 3 are analyzed by a difference velocity across input and output. Consequently, the influence of the phase shift can be summarized in one parameter. According to the investigated phase shifts with gear set 1, the same phase shifts are analyzed. For these cases, the results are shown in Figure 9. Due to the helix angle and the higher total contact ratio, gear set 3 has a lower excitation behavior than gear set 2. For the averaged frequency spectra in the upper row, differences between the two data sets occur. Within the frequency range between $f=1 - 2$ kHz, the variant with phase shift $p=0.5$ has a lower excitation level. Because of the high human sensitivity within this frequency range, these data have to be analyzed by the psychoacoustic metrics at a later date. These differences are confirmed by means of the averaged order spectra. In this case, the gear

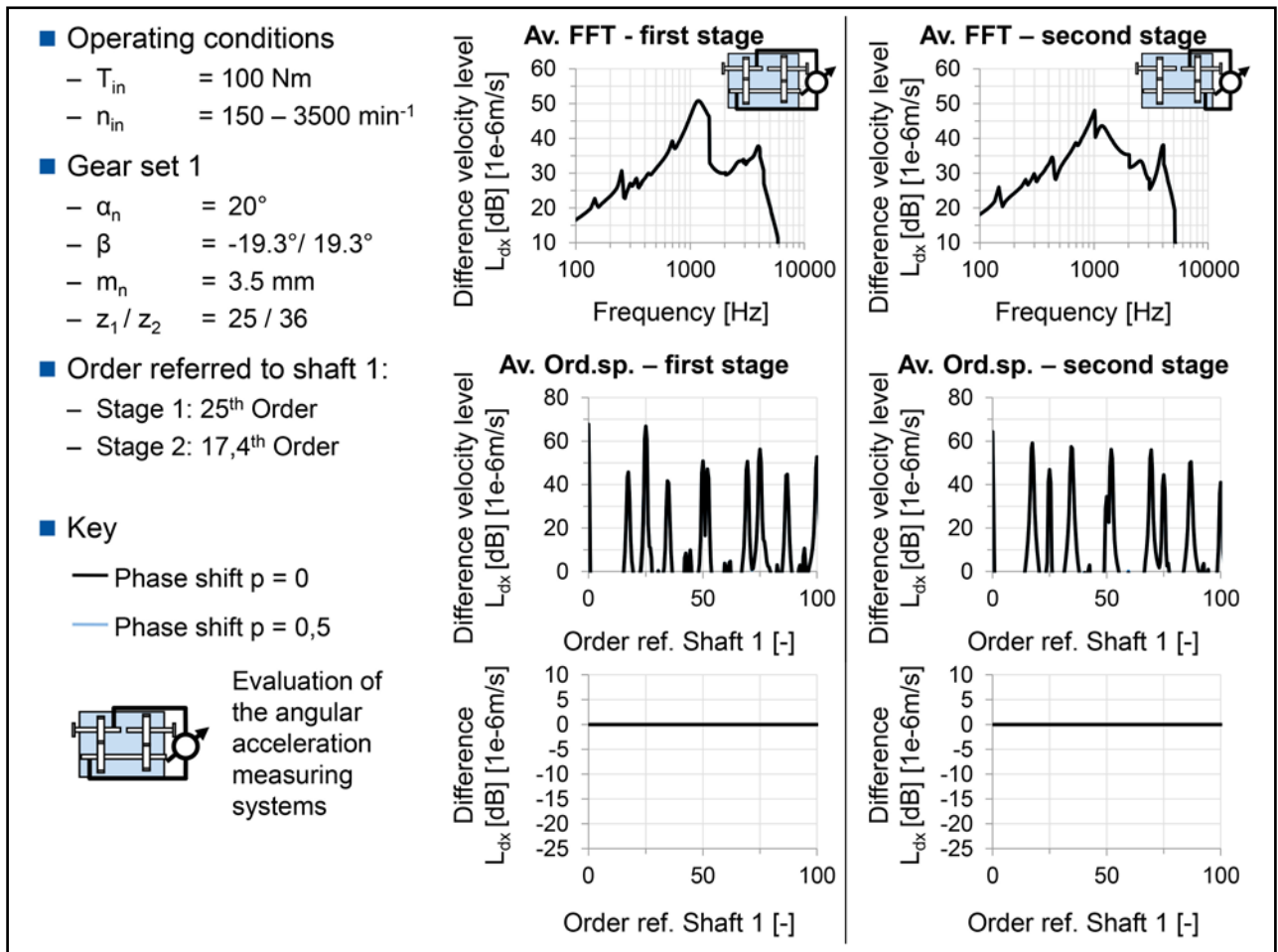


Figure 8 Excitation Behavior of Gear Set 1 with Varied Phase Shift.

mesh order of gear set 2 are the 32nd and of gear set 3 the 30th order. For both gear sets, the excitation level of the first and the third gear mesh order decreases for a phase shift $p=0.5$. In contrast, the second gear mesh order remains the same. The differences of the orders show a difference around 3.5 dB for the first gear mesh order and around 2.5 dB for the third gear mesh order of both gear sets. Hence, the phase shift enables us to reduce torsional vibrations of the drive train.

Summary and Outlook

Nowadays, multi-stage gearboxes are often used due to the need for high ratio gearboxes. Besides current development trends such as electrification and hybridization of the drive train, increased customer requirements and amended law restrictions result in an increased importance of the acoustic behavior. Existing papers show methods to optimize the excitation and noise behavior of single-stage gearboxes. Due to the interactions between the gear meshes, the methods

for noise optimization of single-stage gearboxes cannot be transferred to two-stage gearboxes without restrictions. Among other parameters, the phase shift, the stiffness of the intermediate shaft, and the number of teeth are parameters which influence the excitation behavior. Therefore, the objective of this paper is to analyze the dynamic excitation behavior of two-stage gearboxes with focus on the phase shift.

First, an existing single-stage gearbox is introduced. Furthermore, a two-stage gearbox has been developed and designed which is based on the concept of the single-stage gearbox. Regarding the machine-acoustic noise generation, different measurement equipment is integrated in the test setup. Angular acceleration measurement systems detect the gear mesh excitation. Furthermore, the structure-borne and airborne noise is detected.

Secondly, a simulation model is presented which consists of two main components. The force coupling element represents the gear mesh and a drive train

model based on a torsional multi-body-simulation model. For the single-stage gearbox, the simulation model is validated by means of experimental results. Especially within the acoustic relevant frequency range, experimental and analytical results show a good correlation. Afterwards, the validated model is enhanced to a two-stage model.

With this model, the dynamic excitation behavior is analyzed. Hence, three different gear sets are investigated. The first gear set has a different number of teeth on the intermediate shaft. Therefore, the phase shift has no influence on the excitation behavior. Gear sets 2 and 3 have the same number of teeth on the intermediate shaft. Gear set 2 is a spur, and gear set 3 a helical gear pair. In order to investigate the influence of the phase shift, two different phase shifts are investigated ($p=0, 0.5$). Compared to a simultaneous entering of gear meshes of the two gear stages, a shifted entering of the gear meshes ($p=0.5$) leads to decreased vibration levels of the gear mesh orders.

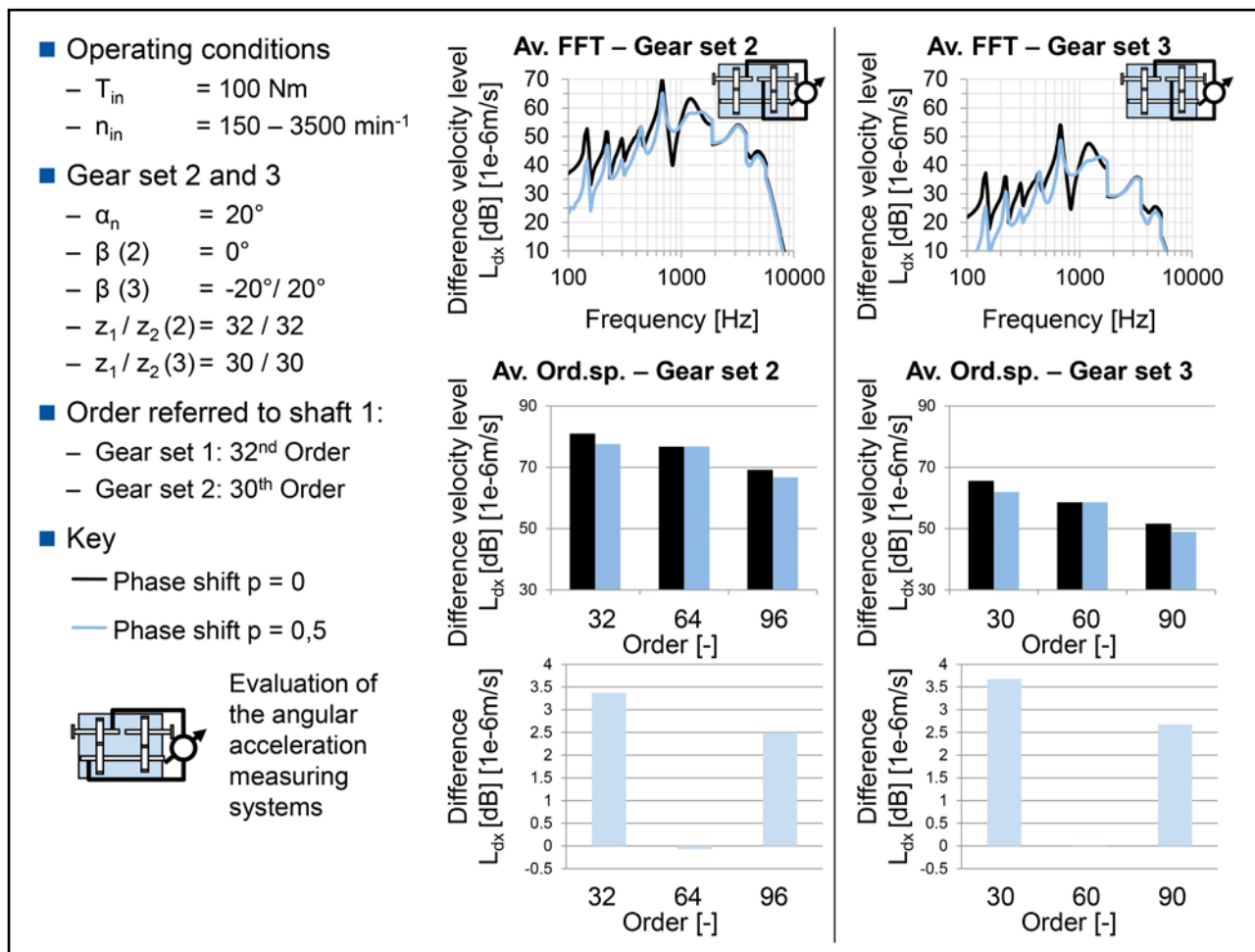



Figure 9 Excitation Behavior of Gear Sets 2 and 3 with Varied Phase Shift.

In the future, the calculated results of the two-stage gearbox model have to be validated experimentally. For that purpose, the two-stage gearbox will be manufactured. Different transfer functions can be obtained by means of the experimental results. On the one hand, the transfer function between the gear mesh excitation and the airborne noise has to be analyzed. On the other hand, the mutual interaction between the gear meshes can be analyzed by a transfer function as well. Furthermore, a detailed parameter study can be performed by calculation based on the validated model. Both experimental and analytical results have to be analyzed with psychoacoustic metrics. The psychoacoustic metrics evaluate noise based on human perception. Consequently, the annoyance of noise can be quantified. 

Acknowledgement. *The authors gratefully acknowledge financial support provided by the German Research Foundation (DFG) (BR 2905/66-1) for the achievement of this project's results.*

References

1. Brecher, C., 2012, Handbuch der FE-Stirnradkette Version 4.2, Werkzeugmaschinenlabor WZL, Aachen.
2. Brumm, M., 2011, "Einflankenwälzprüfung von Hypoidgetrieben", Dissertation, Werkzeugmaschinenlabor (WZL) der RWTH Aachen, RWTH Aachen.
3. Cao, J., 2002, "Anforderungs- und fertigungsgerechte Auslegung von Stirnradverzahnungen durch Zahnkontaktanalyse mit Hilfe der FEM", Dissertation, Werkzeugmaschinenlabor (WZL) der RWTH Aachen, RWTH Aachen.
4. Carl, C.E., 2014, "Gehörbezogene Analyse und Synthese der vibroakustischen Geräuschanregung von Verzahnungen", Dissertation, Werkzeugmaschinenlabor (WZL) der RWTH Aachen, RWTH Aachen.
5. Cheon, G.-J., 2010, "Numerical study on reducing the vibration of spur gear pairs with phasing", Journal of Sound and Vibration.
6. Craig, R. and Bampton, M., Coupling of Substructures for Dynamic Analyses.
7. Richtlinie VDI/VDE, 2001, "Einflanken- und Zweiflanken-Wälzprüfung an Zylinderrädern, Kegelrädern, Schnecken und Schneckenrädern", Richtlinie VDI/VDE 2608.
8. Richtlinie VDI, 1985, "Emissionskennwerte technischer Schallquellen - Getriebe", Richtlinie VDI 2159.
9. Gold, P.W., 1979, "Statisches und dynamisches Verhalten mehrstufiger Zahnradgetriebe", Dissertation, Werkzeugmaschinenlabor (WZL) der RWTH Aachen, RWTH Aachen.
10. Hesse, J., 2011, "Verzahnungsanregung im Antriebsstrang", Dissertation, Werkzeugmaschinenlabor (WZL) der RWTH Aachen, RWTH Aachen.

11. Hohle, A.C., 2002, "Auswirkungen von Rauheit Oberflächenstruktur und Fertigungsabweichung auf das Lauf- und Geräuschverhalten hartfeinbearbeiteter hochüberdeckender Zylinderräder", Dissertation, Werkzeugmaschinenlabor (WZL) der RWTH Aachen, RWTH Aachen.
12. Kubur, M. and Kahraman, A. and Zini, D.M. and Kienzle, K., 2004, "Dynamic Analysis of a Multi-Shaft Helical Gear Transmission by Finite Elements", Journal of Vibration and Acoustics.
13. Landvogt, A., 2003, "Einfluss der Hartfeinbearbeitung und der Flankentopographieauslegung auf das Lauf- und Geräuschverhalten von Hypoidverzahnungen mit bogenförmiger Flankenlinie", Dissertation, Werkzeugmaschinenlabor (WZL) der RWTH Aachen, RWTH Aachen.
14. Marquardt, R., 1995, "Einflankenwälzprüfung", wt-Produktion und Management.
15. Möllers, W., 1982, "Parametererregte Schwingungen in einstufigen Zylinderradgetrieben", Dissertation, RWTH Aachen.
16. Müller, R., 1991, "Schwingungs- und Geräuschanregung bei Stirnradgetrieben", Dissertation, Institut für Konstruktions-, Produktions- und Arbeitswissenschaften, TU München.
17. Salje, H., 1987, "Optimierung des Laufverhaltens evolventischer Zylinderrad-Leistungsgetriebe", Dissertation, Werkzeugmaschinenlabor (WZL) der RWTH Aachen, RWTH Aachen.
18. Sattelberger, K., 1997, "Schwingungs- und Geräuschanregung bei ein- und mehrstufigen Stirnradgetrieben", Dissertation, TU München.
19. Umweltbundesamt, 16.02.2016, "Verkehrslärm", www.umweltbundesamt.de/themen/verkehr-laerm/verkehrsplaerm/strassenverkehrsplaerm.
20. Vinayak, H. and Singh, R. and Padmanabhan, C., 1995, "Linear dynamic analysis of multi-mesh transmissions containing external, rigid gears", Journal of Sound and Vibration.
21. DIN EN IEC, 2007, "Windenergieanlagen - Teil 11: Schallmessverfahren", DIN EN IEC 61400-11.
22. Zhou, C. and Young, S. and Tang, Y., "Two-stage Gear Driveline Vibration and Noise."
23. Ziegler, H., 1971, "Verzahnungssteifigkeit und Lastverteilung schrägverzahnter Stirnräder", Dissertation, WZL, RWTH Aachen.

For Related Articles Search

noise

at www.geartechnology.com

Marius Schroers, M.Sc., studied mechanical engineering at RWTH Aachen University till 2015. Since that time, he works as a scientific research assistant in the group "Gear Design and Manufacturing Simulation" in the gear department of the Laboratory of Machine Tools and Production Engineering (WZL). His research activities are focused on the dynamic behavior of multi-stage gearboxes and the correlation between excitation, noise radiation and the perception related evaluation of gearbox noise.



Dr.-Ing. Dipl.-Wirt.-Ing. Christoph Löpenhaus is a 2010 industrial engineering graduate of RWTH Aachen; he received his Ph.D. (local strength and friction models for gears) in 2015. Upon graduation he worked as a research assistant in the gear testing group of the Laboratory for Machine Tools (WZL) of RWTH Aachen and in 2011 was named the group's team leader. Löpenhaus has since 2014 worked as chief engineer of the department for gear technology at WZL.



Prof. Dr.-Ing. Christian Brecher has since January 2004 been Ordinary Professor for Machine Tools at the Laboratory for Machine Tools and Production Engineering (WZL) of the RWTH Aachen, as well as Director of the Department for Production Machines at the Fraunhofer Institute for Production Technology IPT. Upon finishing his academic studies in mechanical engineering, Brecher started his professional career first as a research assistant and later as team leader in the department for machine investigation and evaluation at the WZL. From 1999 to April 2001, he was responsible for the department of machine tools in his capacity as a Senior Engineer. After a short spell as a consultant in the aviation industry, Professor Brecher was appointed in August 2001 as the Director for Development at the DS Technologie Werkzeugmaschinenbau GmbH, Mönchengladbach, where he was responsible for construction and development until December 2003. Brecher has received numerous honors and awards, including the Springorum Commemorative Coin; the Borchers Medal of the RWTH Aachen; the Scholarship Award of the Association of German Tool Manufacturers (Verein Deutscher Werkzeugmaschinenfabriken VDW); and the Otto Kienzle Memorial Coin of the Scientific Society for Production Technology (Wissenschaftliche Gesellschaft für Produktionstechnik WGP).

